

This article was downloaded by:

On: 21 January 2011

Access details: *Access Details: Free Access*

Publisher *Taylor & Francis*

Informa Ltd Registered in England and Wales Registered Number: 1072954 Registered office: Mortimer House, 37-41 Mortimer Street, London W1T 3JH, UK



The Journal of Adhesion

Publication details, including instructions for authors and subscription information:

<http://www.informaworld.com/smpp/title~content=t713453635>

Evaluating the Rate-Dependent Fracture Toughness of an Automotive Adhesive

D. J. Pohlit^a; D. A. Dillard^a; G. C. Jacob^b; J. M. Starbuck^c

^a Engineering Science and Mechanics Department, Virginia Tech, Blacksburg, VA, USA ^b Materials Science and Engineering Department, University of Tennessee, Knoxville, TN, USA ^c Senior Research Staff, Polymer Matrix Composites Group, Material Science & Technology Division, Oak Ridge National Laboratory, Oak Ridge, TN, USA

To cite this Article Pohlit, D. J. , Dillard, D. A. , Jacob, G. C. and Starbuck, J. M.(2008) 'Evaluating the Rate-Dependent Fracture Toughness of an Automotive Adhesive', *The Journal of Adhesion*, 84: 2, 143 – 163

To link to this Article: DOI: 10.1080/00218460801952825

URL: <http://dx.doi.org/10.1080/00218460801952825>

PLEASE SCROLL DOWN FOR ARTICLE

Full terms and conditions of use: <http://www.informaworld.com/terms-and-conditions-of-access.pdf>

This article may be used for research, teaching and private study purposes. Any substantial or systematic reproduction, re-distribution, re-selling, loan or sub-licensing, systematic supply or distribution in any form to anyone is expressly forbidden.

The publisher does not give any warranty express or implied or make any representation that the contents will be complete or accurate or up to date. The accuracy of any instructions, formulae and drug doses should be independently verified with primary sources. The publisher shall not be liable for any loss, actions, claims, proceedings, demand or costs or damages whatsoever or howsoever caused arising directly or indirectly in connection with or arising out of the use of this material.

Evaluating the Rate-Dependent Fracture Toughness of an Automotive Adhesive

D. J. Pohlit^{1,*}, D. A. Dillard¹, G. C. Jacob^{2,**},
and J. M. Starbuck³

¹Engineering Science and Mechanics Department, Virginia Tech, Blacksburg, VA, USA

²Materials Science and Engineering Department, University of Tennessee, Knoxville, TN, USA

³Senior Research Staff, Polymer Matrix Composites Group, Material Science & Technology Division, Oak Ridge National Laboratory, Oak Ridge, TN, USA

Adhesives have made significant inroads into structural bonding of automobiles, but concerns remain over the integrity of these bonds under high speed loading conditions that could occur in accidents. A commercial epoxy adhesive is characterized over a wide range of crosshead rates using compact tension fracture specimens made of the neat resin. Measured fracture toughness values at room temperature decreased steadily from 2.5 MPa \sqrt{m} to roughly 1.7 MPa \sqrt{m} as crosshead speeds increased from 10^{-6} to 1 m/s, exhibiting similar behavior as observed in tests of bonded double cantilever beam tests reported elsewhere. Additionally, intermediate rate tests conducted at subambient temperatures showed fracture toughness values that were comparable with the high rate tests conducted at room temperature. Applications of time temperature superposition principle techniques may be suitable for predicting the fracture behavior of the adhesive studied herein. Good correlation was also found between the fracture toughness values measured and the value of $\tan \delta$ obtained from dynamic mechanical analysis tests conducted at the corresponding reduced test rate.

Keywords: Compact tension specimen; Epoxy adhesive; Fracture energy; Fracture toughness; High speed fracture; Impact; Rate-dependent fracture; Time dependence; Time temperature superposition

Received 9 May 2007; in final form 21 January 2008.

*Present address of David J. Pohlit is: Naval Surface Warfare Center, Carderock Division, Bethesda, Maryland, USA.

**Currently a Senior Research Engineer at the Dow Chemical Company, Freeport, Texas.

Address correspondence to David A. Dillard, Department of Engineering Science and Mechanics, Virginia Tech, Blacksburg, VA 204361-0219, USA. E-mail: dillard@vt.edu

INTRODUCTION

Adhesives are used increasingly for many automotive applications, including joining of structural components. Long advocated for weight savings, reductions in noise, vibration, and harshness (NVH), sealing capabilities, and improved fatigue resistance, adhesives have become an essential means of assembling automobiles and other transportation vehicles. Modern dispensing equipment and robots, newer adhesives, and improved cure techniques have contributed to their ease of application and reductions in joining cost. New opportunities for adhesive bonding are resulting from the quest for lighter weight and more energy efficient automobiles, where hybrid structures often require joining dissimilar materials, and applications where spot welding and mechanical fastening become impractical or impossible. As adhesives take on more significant roles in automobile assembly, their durability and performance over a range of environmental and loading scenarios is of significant concern. This paper will address characterizing the impact fracture behavior of a commercial adhesive that has been marketed to the automotive industry for model development and possible utilization. A general background for impact fracture testing of polymers and other materials may be found in useful references [1–3].

A number of test methods have been advanced to measure the fracture toughness or fracture energy of adhesives for many applications. Neat resin adhesive samples may be characterized just as other polymers, using common configurations such as compact tension (CT) or single edge notch bend (SENB) specimens. Quasi-static test standards exist for these geometries and practitioners have extended the methods to higher rates of testing [4]. The SENB specimen appears to be more popular in the literature for characterizing the impact behavior of polymers, perhaps because of the convenience of performing such tests in drop towers. However, the CT specimen has also been used in conjunction with high-rate servo-hydraulic test frames when a wider range of test rates is desired [4,5].

Since adhesives will typically be used in the joining of substrates, fracture tests of bonded joints are also popular. Although linear elastic constitutive properties are often similar for neat resin and bonded joints, behavior beyond yielding, including strength and fracture properties, are often quite distinct. For structural applications of interest here, beam type fracture specimens are common, including the double cantilever beam (DCB) for Mode I loading, the end notched flex (ENF) or end loaded split (ELS) for Mode II loading, and the single leg bend (SLB), also known as the mixed mode flex (MMF), for mixed Mode I/II characterization. The adhesive studied herein has also been

characterized using bonded specimens as well [6–10]. Significant stick slip behavior was seen at both quasi-static and low-speed impact test rates, suggesting considerable rate dependence of the material.

Applications of the time temperature superposition principle (TTSP) to constitutive behavior of polymers has been widely used, and with great success, to predict behavior at much shorter or longer times than are experimentally accessible [11]. Provided the polymer does not change during testing or service, temperature-dependent shift factors may be used to scale times for accurate predictions. Failures of TTSP for modeling constitutive properties are occasionally observed when chemical, morphological, or physical changes occur in a polymer during the testing or actual service conditions. The literature contains numerous successful examples of applying TTSP to other polymer properties such as strength and fracture behavior for a range of adhesive materials [12,13].

MATERIALS AND SPECIMEN PREPARATION

The adhesive used, PL731SI, is a commercially available, two-part epoxy system (Sovereign Specialty Chemicals, Inc., Chicago, IL, USA). The resin and hardener were mixed at a 4:1 ratio using a MixPac MC 10–24 static mixer (MixPac Systems AG, Rotkreuz, Switzerland) on a Profill pneumatic dispenser (Profill Corp., North Canton, OH, USA). The adhesive was degassed by centrifuging for 15 min at room temperature in a container that could serve as a syringe for subsequent dispensing. The adhesive was then carefully squeezed onto a stainless steel plate that had been coated with Lilly RAM 225 (RAM Chemicals, Gardena, CA, USA) mold release to allow for subsequent separation. A dam of silicone rubber tubing and rigid spacers of the desired thickness were used to support a second plate to produce a plaque with consistent thickness. The plates were clamped together and the assembly was held at 125°C for 60 min in a convection oven. The curing procedure was used based on discussions with the manufacturer. Using this technique, neat adhesive plaques were prepared with thicknesses of 8 mm.

After curing, specimens were cut from the plaques with a milling machine, using water as the cutting fluid. CT specimens were fabricated according to ASTM D-5045 [14] and appropriately sized to the recommended dimensions for a thickness of 8 mm. Notches were sawn into the samples with a high speed steel (HSS) slitting saw to a depth of $0.45 a/W$, the standard's minimum acceptable crack length, where a is the crack length and W is the depth of the specimen. Pre-cracks

were introduced in some specimens to a distance to exceed twice the cutter radius by tapping with a razor, a method that has been shown to produce lower fracture toughness values [15]. Completed specimens were typically held for a minimum of 7 days in a conditioned laboratory environment prior to testing.

Tensile dogbone specimens were prepared in a similar fashion with a thickness of 3 mm. Blanks were cut from the plaques and then machined to the ASTM D-638 standard shape using a Tensilkut model 10–21 specimen router (Tensilkut Engineering, Maryville, TN, USA). These specimens were used to determine the modulus and yield properties of the adhesive. Dynamic mechanical analysis specimens were also cut from these plaques for thermal analysis.

FRACTURE TESTING METHODOLOGY

Experimental Set-up

An MTS servo-hydraulic machine (MTS Corporation, Eden Prairie, MN, USA) equipped with a 50 kN actuator and two 1 liter/sec servo valves was used for initial rounds of testing at speeds up to 1 m/s. A 5000 N strain gage-based load cell was initially used for acquiring load measurements. Data were acquired at sampling rates of up to 33,000 samples per second using a PCI-6031E National Instruments data acquisition card in a computer running custom LabVIEW (National Instruments, Austin, TX, USA) software. The strain gage-based load cell led to anomalous load values at the higher loading rates, as has been experienced by others [2,16]. Subsequent testing was performed on a higher speed load frame that was equipped with a 40 kN piezoelectric load cell that offered a much faster response time. This MTS servo-hydraulic machine was capable of achieving test velocities up to 18 m/s, and included two 190-liter accumulators and a 25.2 liter/s main servo valve. Additionally, this load frame was controlled using custom LabVIEW data acquisition software capable of achieving sampling rates up to 100,000 samples per second. The higher sensitivity and faster response time of the piezoelectric load cell allowed for consistent load data to be collected.

Modifications to the load trains of both test machines were made to improve results for the higher rate CT tests. In order to minimize the mass of the load train between the specimen and load cell, a short section of threaded rod was used to attach a small aluminum clevis directly to the load cell, which was in turn mounted to the upper, stationary crosshead. The lower clevis was attached to a small slack adaptor (also known as a lost motion device) to allow the actuator to

reach the set-point velocity prior to engaging the specimen. Self-locking tapers have been used to minimize anomalous ringing of the load train. For the purpose of this study, a small slack adaptor was fabricated by cutting a #2 Morse taper extension in half, threading the ends appropriately, and assembling into an inexpensive unit, as illustrated in Fig. 1, for the initial round of dynamic testing. The device provided sufficiently smooth loading profiles, especially when a small amount of lubricant was added to prevent premature sticking. Additionally, an alternative design was utilized for the second round of dynamic testing on the faster servo-hydraulic test machine. This design made use of a small, off-the-shelf linear ball bearing combined with a 6.35 mm diameter stainless steel rod and custom-machined aluminum housing to provide an adequate travel distance for test velocities up to 10 m/s prior to engaging the test specimens. A schematic of the modified load train utilized in the second round of testing is illustrated in Fig. 2.

Data Analysis

For common fracture specimens, the Mode I stress intensity factor is given by:

$$K_I = \frac{F}{B\sqrt{W}} \cdot f\left[\frac{a}{W}\right], \quad (1)$$



FIGURE 1 Simple slack adaptor components fabricated from a #2 Morse taper extension, as shown at the top.

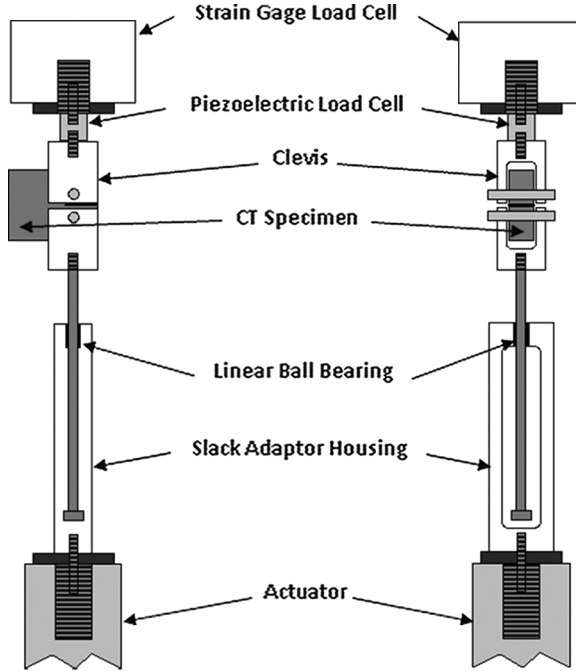


FIGURE 2 Modified load train used for dynamic CT tests.

where F is the applied load, B is the specimen thickness, W is the specimen width, a is the crack length, and f is a function of the non-dimensional crack length, a/W . For intermediate crack lengths in the CT specimen, f may be approximated as [14]:

$$f\left[\frac{a}{W}\right] = \frac{2 + \left(\frac{a}{W}\right)}{\left(1 - \left(\frac{a}{W}\right)\right)^{\frac{3}{2}}} \left[0.886 + 4.64\left(\frac{a}{W}\right) - 13.32\left(\frac{a}{W}\right)^2 + 14.72\left(\frac{a}{W}\right)^3 - 5.6\left(\frac{a}{W}\right)^4 \right]. \quad (2)$$

Following the ASTM D 5045** standard, a conditional fracture toughness, K_Q , is defined for $F = F_{\max}$ when the load trace is linear to failure or when nonlinear behavior is evident in the load-deflection trace, using the intercept of the trace and a line drawn at 95% of the linear slope, F_Q . Provided the characteristic dimensions (W , a , and ligament length) of the specimen are sufficiently large compared with the

**A reviewer pointed out that ISO 17281 addresses similar testing configurations and is advocated at rates up to 1 m/s.

plastic zone size at the tip of the crack, a valid plane strain fracture toughness value is obtained as $K_{Ic} = K_Q$. This three-fold size requirement is expressed as:

$$B, a, (W - a) > 2.5 \left(\frac{K_Q}{\sigma_y} \right)^2, \quad (3)$$

where σ_y is the yield strength of the material. If these criteria are not satisfied, larger specimens must be tested to obtain a valid linear elastic fracture mechanics (LEFM) parameter. These criteria are often considered to be conservative, so comparisons of specimens that deviate somewhat from these criteria may still be possible [5].

The results presented herein will focus on the effect of applied crosshead rate on measured fracture toughness values. However, in using these results for numerical modeling of the rate dependence of the fracture behavior, the need arose for an effective measure of the crack tip loading rate. A meaningful measure of loading rate is the time rate of change of the applied stress intensity factor, dK_I/dt , where all the quantities except the applied force in Eq. (1) are assumed to be constant during the loading event prior to catastrophic crack propagation. The time to failure is also commonly used as a rate parameter. For this paper we will report both the crosshead rate, a prescribed test parameter, as well as dK_I/dt , which we believe to be more physically meaningful as a local crack-tip loading rate.

EXPERIMENTAL RESULTS

Ambient Temperature CT Tests

In earlier fracture testing of DCB specimens consisting of aluminum and composite adherends bonded with the PL731SI adhesive, cohesive failures within the adhesive layer showed dramatic stick-slip behavior [6,7], suggesting a strong time dependence. This time dependence, coupled with an interest in properties under both quasi-static and impact conditions, led to the development of a relevant test matrix. The neat adhesive fracture tests conducted in this study were tested over a wide range of test rates ranging from 10^{-6} to 1 m/s. Tests were conducted at room temperature, as well as at several different subambient temperatures. Lower temperatures were chosen because of their correlation with high-rate testing through the TTSP, as will be discussed in the next section.

Figure 3 illustrates the measured fracture toughness values obtained from room temperature tests as a function of applied crosshead rate.

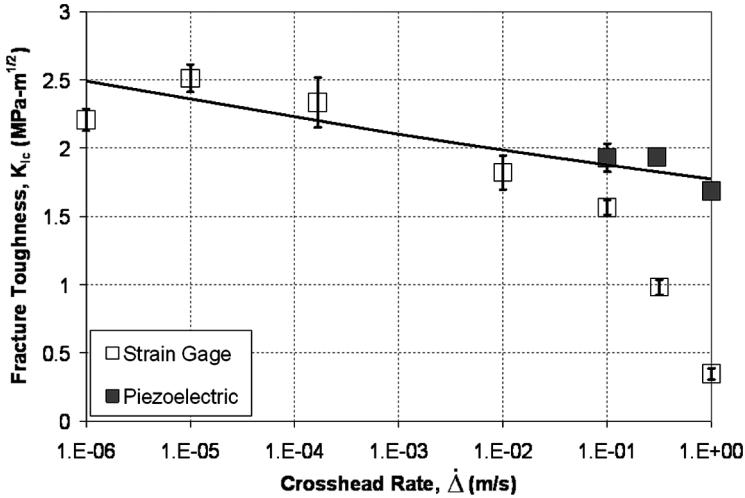


FIGURE 3 Measured fracture toughness values as a function of crosshead rate for tests conducted with strain gage-based and piezoelectric load cells. Error bars for two highest rates (*i.e.* 0.3 and 1 m/s) are so small that they are hidden for piezoelectric load cell (shaded symbols) results.

Two or three specimens were tested for most conditions, and data were quite consistent, as evidenced by the error bars representing one standard deviation from the mean. The small sample size seemed appropriate because of the very repeatable results observed at all crosshead rates. At the highest loading rates, substantial differences are noted between the results from the strain gage-based and piezoelectric load cells to show the substantial errors that can be introduced if the response time of the load sensor is inadequate.

With the exception of the result at the slowest rate (10^{-6} m/s), a consistent downward trend is observed in the fracture toughness values as the crosshead rate is increased over the full range of data. At the three slower rates, significant stress whitening was observed in the failed specimens, and the plane strain fracture toughness, K_{Ic} , was determined from the intercept of a 95% slope with the load trace [14]. This corresponds to limited subcritical crack growth prior to catastrophic rupture. At higher rates, failures were more brittle and the fracture toughness values were determined from the peak load and the linearity of the load trace did not suggest subcritical crack growth.

As the higher crosshead rates were approached, the peak loads obtained with the strain gage-based load cell dropped precipitously, and the symmetric load traces suggested significant inertial effects.

Clearly the values obtained were well below the values obtained with the piezoelectric load cell with the faster response time. Concerns with load cell response time, anomalous load traces, and fracture toughness values that fell well below those obtained at subambient temperatures and failed to correspond with fracture energies obtained on DCB tests of bonded specimens, all suggested that the loads obtained with the strain gage-based load cells were in error. On the other hand, the results obtained from the piezoelectric load cell seemed to satisfy these concerns and led to internally consistent results. Consequently, the remaining results presented in this paper will focus on the piezoelectric load cell results.

As will be shown later, a correlation between these bulk CT data and results obtained on bonded DCB specimens has been made. Because of the different loading kinetics, attempts to compare results from CT and DCB tests must recognize the effective rate of loading at the crack tip. When considering the nature of each type of test specimen, it is clear that the CT specimens experience a very short time to failure due to the high relative stiffness of such a test specimen. In contrast, the bonded beam specimens experience rather large deformations and, thus, undergo a much larger period of loading due to their relative flexibility [8]. Using a common fracture mechanics approach, the effective fracture loading rate, dK/dt , is often used, where K is the stress intensity parameter and dt refers to the time to failure for a particular fracture event. Therefore, the same data illustrated in Fig. 3, but now plotted in terms of crack tip loading rate, dK_I/dt , are shown in Fig. 4.

Subambient Temperature and Dynamic Mechanical Analysis(DMA)

Dramatic drops in fracture toughness at higher test rates were suggested from the initial round of testing conducted with the strain gage-based load cell, as observed in Fig. 3. Subambient temperature tests were then conducted to determine if TTSP could be used to infer behavior at even higher loading rates. To correlate the subambient test results to different loading rates, DMA tests were conducted. Small single-cantilever beam specimens were cut from the cured adhesive plaques and were evaluated using the DMA method to determine the glass transition temperature of the adhesive. The glass transition temperature, T_g , was determined to be about 100 and 125°C, based on the peaks of the E'' and $\tan \delta$ curves, respectively, at a frequency of 1 Hz. The DMA results for a typical sample subjected to a temperature sweep are shown in Fig. 5.

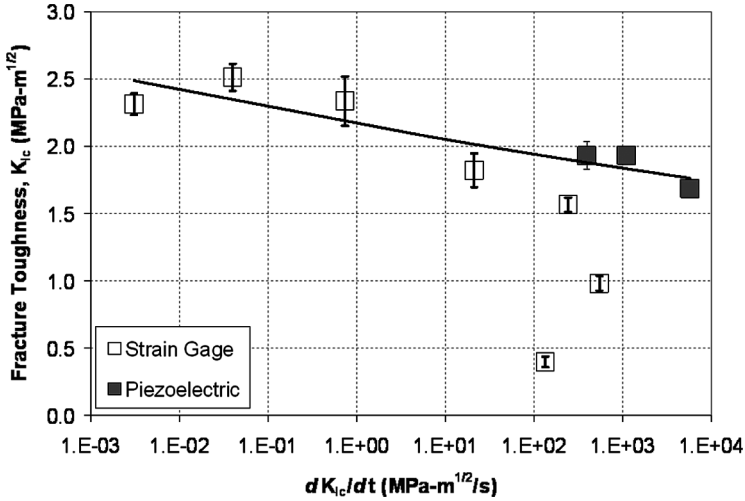


FIGURE 4 Measured fracture toughness values as a function of dK_{Ic}/dt for tests conducted with strain gage-based and piezoelectric load cells. Error bars for two highest rates (*i.e.* 0.3 and 1 m/s) are so small that they are hidden for piezoelectric load cell (shaded symbols) results.

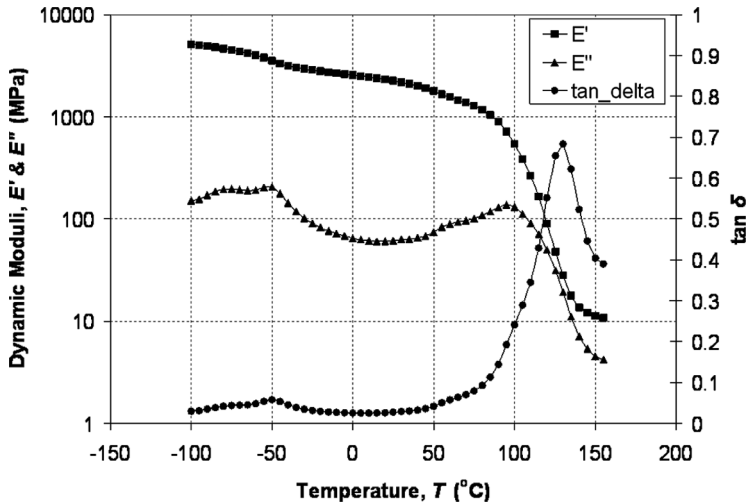


FIGURE 5 DMA results at 1 Hz for bulk adhesive sample measured with a temperature sweep.

The dynamic moduli results obtained over a range of temperatures and at frequencies of 0.1, 0.2, 0.5, 1, 2, 5, 10, and 20 Hz were shifted, thus establishing the corresponding shift factors to be used in the generation of a master curves for the DMA measured properties. Figure 6 illustrates the resulting shift factor plot for the dynamic moduli. Some differences were seen in the shift factors, with the values obtained from the loss moduli showing more erratic behavior. A linear relationship was developed for later use by relating the storage modulus shift factor, a_T , and temperature, T :

$$\log(a_T) = -0.1601T + 5.24. \quad (4)$$

Figure 7 provides the master curves resulting from the use of the common shift factor approximation provided in Eq. (4) for both dynamic moduli as well as the $\tan \delta$ results.

Figure 8 illustrates a fracture toughness master curve ($T_{ref} = 25^\circ\text{C}$) obtained by combining the room temperature and subambient temperature test results. The subambient temperature results have been shifted to their corresponding test rates by using the relationship provided in Eq. (4). In short, these results have been shifted by a factor of approximately $5^\circ\text{C}/\text{decade}$ rate of test. Tests conducted at slower rates at temperatures as low as -115°C showed slightly lower fracture toughness values than obtained at room temperature-but, based on

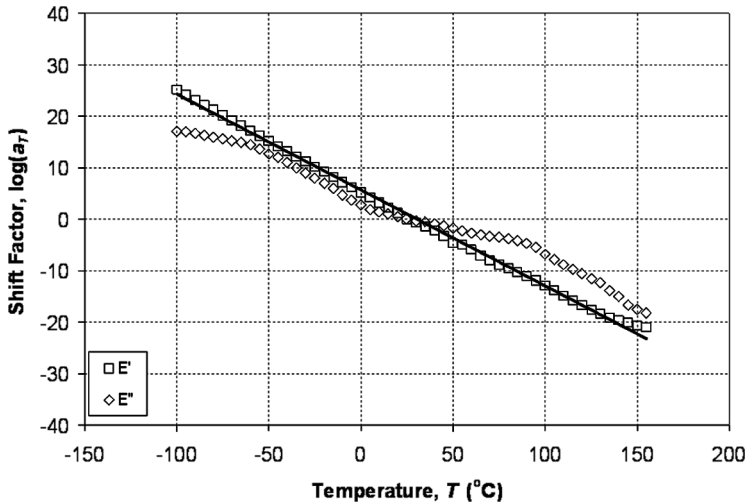


FIGURE 6 Shift factor plot for dynamic moduli results from DMA tests conducted on bulk adhesive sample.

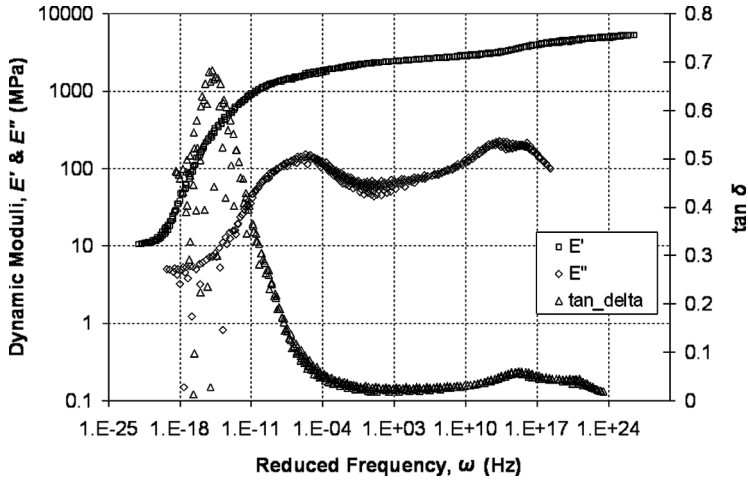


FIGURE 7 Master curves generated from DMA test results on bulk adhesive ($T_{ref} = 25^{\circ}\text{C}$).

these limited results, a glassy plateau appears to be developing after appropriate horizontal shifting is applied. These tests conducted at temperatures of -115 to -40°C and at several displacement rates

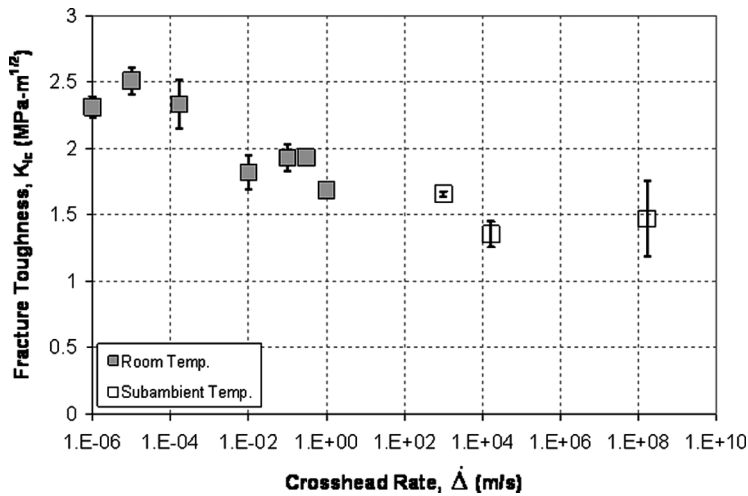


FIGURE 8 Fracture toughness master curve obtained from various cross-head rate data collected at room and subambient temperatures ($T_{ref} = 25^{\circ}\text{C}$). (Error bars for two highest measured rates (*i.e.* 0.3 and 1 m/s) are hidden for room temperature (shaded symbols) results).

showed no specific trends and averaged about $1.4 \text{ MPa} \sqrt{m}$, slightly less than the high rate tests conducted at room temperature. Finally, according to Fig. 8, the trends observed at subambient temperatures for relatively low applied crosshead rates appear to be consistent with the use of TTSP, potentially suggesting that this may be a useful method for characterizing this material.

DISCUSSION

Fracture Surface Morphology

All specimens except those tested at 10^{-6} m/s exhibited unstable catastrophic crack growth. At this slowest rate, stable propagation was observed and the specimens were finally broken manually due to the excessive length of the test. A comparison of the stress-whitened, plastic zones is shown in Fig. 9 for representative samples tested at room temperature over the full range of applied crosshead rates.

The radius of the plastic zone under plane strain conditions may be estimated as:

$$r_p = \frac{1}{6\pi} \left(\frac{K_{Ic}}{\sigma_y} \right)^2. \quad (5)$$

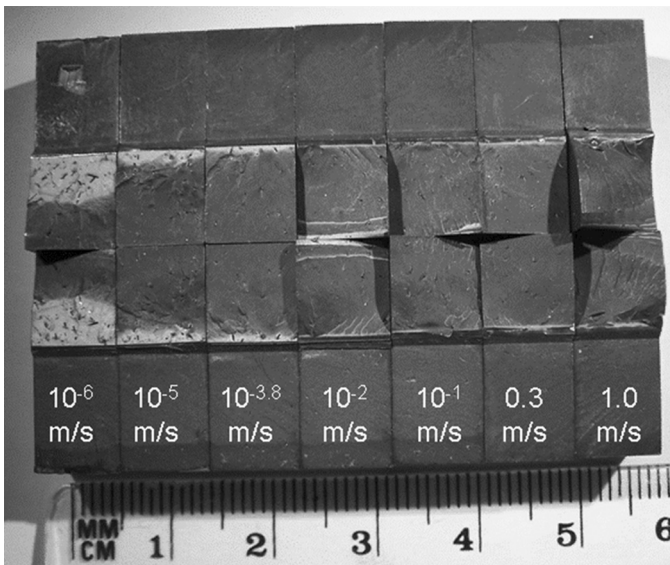


FIGURE 9 Illustration of typical stress whitening for a range of applied crosshead rates.

Dogbone tensile specimen results suggested that the yield stress was on the order of 40 MPa, and showed a modest dependence on crosshead rate [17]. Based on these results, the plastic zone radius would drop from approximately 0.2 mm to about 0.1 mm as the fracture toughness drops from 2.5 to 1.7 MPa \sqrt{m} . Plane strain dimensional requirements were satisfied for all but the slowest test rates.

Figures 10 and 11 provide SEM images of the fracture surfaces of the CT specimens tested at quasi-static and high rates, respectively. Figure 10 shows significant stress whitening taking place ahead of the crack tip due to plastic deformation for a specimen tested at 10^{-6} m/s. Figure 11 illustrates the striations or chevrons on the fracture surface of a specimen tested at an intermediate rate of 0.01 m/s. Note that the plastic deformation ahead of the crack tip is severely limited at this intermediate rate, causing the size of the visible stress-whitened zone to be significantly reduced.

Small stress-whitened zones were observed ahead of the crack tip for all specimens, even at the highest crosshead rates and coldest test temperatures. This was confirmed from the SEM images of the fracture surfaces of specimens tested at the highest crosshead rate of 1 m/s. One concern was whether this observed plasticity could have

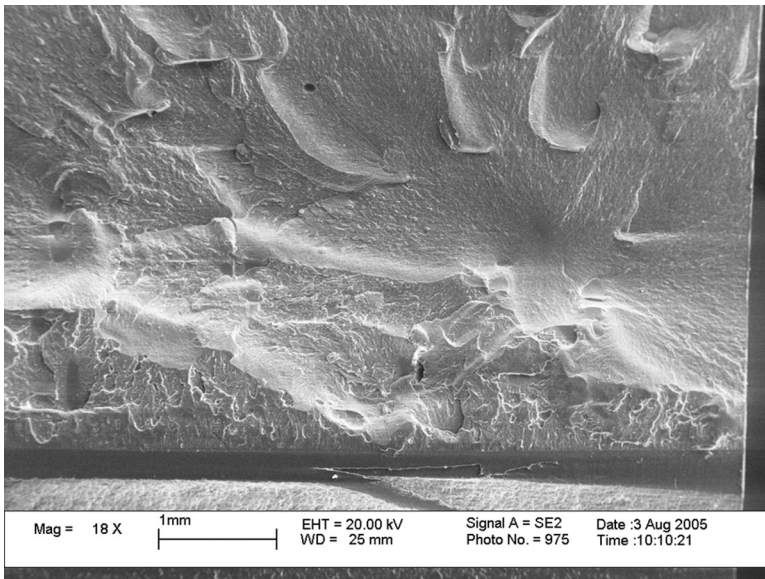


FIGURE 10 SEM image of the fracture surface of a CT specimen tested at a slow rate of 10^{-6} m/s.

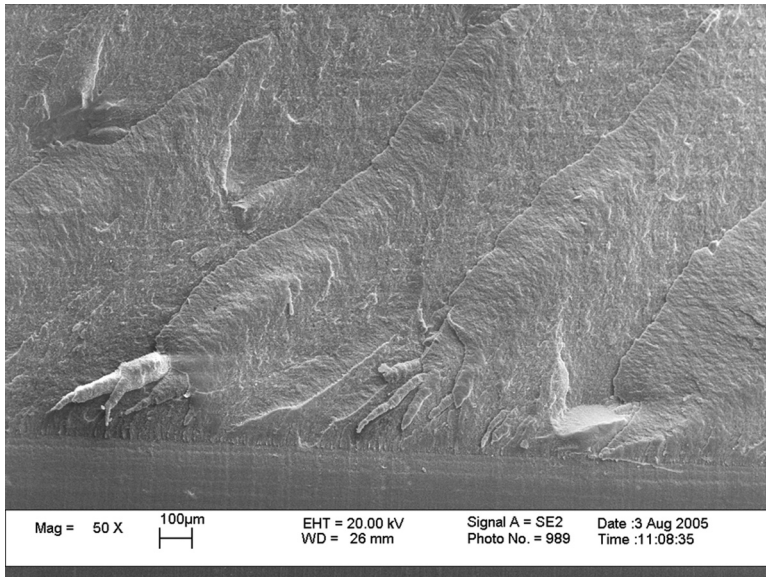


FIGURE 11 SEM image of the fracture surface of a CT specimen tested at an intermediate rate of 0.01 m/s.

been introduced at the crack tip when the cracks were initiated by tapping a razor into the notched specimens. This was especially of concern since the crack tip advanced only a small distance ahead of the razor blade tip—no significant jumps occurred during pre-cracking. To investigate this possibility, several specimens were cooled to -115°C and the crack was advanced by tapping a razor blade. Usually the crack propagated a limited amount, although in one specimen, the crack jumped forward by 13 mm. All of these specimens that were pre-cracked cold continued to show similar amounts of stress whitening at the crack tip and fracture toughness values, leading to the conclusion that stress whitening and the measured fracture toughnesses were not affected by the creation of a pre-crack with a razor blade.

Of some interest is the observation that stress whitening was evident at crack initiation in all specimens, but was not evident in regions where the crack grew rapidly in either the CT specimens or bonded DCB specimens [6,7]. High-speed video recordings of the fractures were made with a Photron FASTCAM APX-RS camera (Photron USA, Inc., San Diego, CA, USA) at framing rates as high as 20,000 fps. In the CT specimens, crack advance occurred within a single frame, suggesting speeds in excess of 200 m/s. (Often seen as an

upper bound for crack propagation, the Rayleigh wave speed for the SIA adhesive is estimated to be 300 m/s). Although stress whitening is evident when a stationary crack is loaded to catastrophic fracture at even the highest crosshead rate, such visual evidence of plasticity is lacking at rapidly moving crack tips.

Correlation with DCB Tests

In a coordinated study conducted on the same adhesive studied herein [7], bonded DCB specimens were tested under quasi-static and dynamic loading conditions. The adhesive exhibited extensive stick-slip behavior for all crosshead rates when bonded graphite/epoxy composite adherend specimens were tested at room temperature. Measured fracture energies for initiation in quasi-static tests averaged from 2450 to 2800 J/m², depending on the adherend thickness. This variation appears to be largely due to the longer time required for crack propagation in thinner and less stiff adherends, as a constant crosshead rate was used for all specimens. Upon initiation, the debond would jump forward by 50 mm or more, resulting in apparent arrest values as low as 150 J/m². Such arrest values have long been viewed with suspicion since kinetic energy during rapid crack growth can drive the crack beyond what might be predicted based on static equations [18,19]. Nonetheless, the decreases in applied fracture energy do suggest a strong dependence on rate. Additionally, average fracture energies during the debond events were on the order of 600 to 800 J/m², again depending on the adherend thickness [7].

As mentioned earlier, a correlation has been made between the fracture results obtained from bulk adhesive CT tests and bonded DCB specimens. However, instead of analyzing the K_{Ic} of the two different specimen geometries, the strain energy release rate (G_{Ic}) has been utilized as this is a more common fracture parameter for adhesive joints involving dissimilar materials. Therefore, the fracture toughness results obtained from the CT tests presented herein have been converted to strain energy release rate values for comparison purposes by using the following relationship:

$$G = \frac{K^2(1 - \nu^2)}{E}, \quad (6)$$

where ν and E are the Poisson's ratio, 0.38, and elastic modulus, 2.3 GPa, of the adhesive material, respectively. Questions could be raised regarding the effect of the imposed adherend constraints on the resulting plastic zone size relationship to adhesive thickness,

which has been addressed in previous studies [20,21]. Calculations corresponding to the various rates of tests have been shown to produce plastic zone sizes less than the total bond-line thickness utilized in a study of bonded composite joints [6].

It should be noted that a previous study [17] has shown a slight variation in the elastic modulus over the range of applied loading rates discussed herein. In particular, the modulus was shown to increase from 2.2 to 2.37 GPa over the range of applied crosshead rates of 0.1 to 100 mm/min. This data were used to perform a linear extrapolation to determine modulus values corresponding to the range of applied crosshead rates of interest for this study. Therefore, calculations were made to determine the effect of the rate-dependent modulus contribution to the calculated strain energy release rate values; however, only small differences were observed, as illustrated in Fig. 12. Results obtained from three different adhesively bonded joint configurations [8] have proven to yield very similar trends as a function of applied crosshead rate to those observed as a result of the study presented herein. Fig. 12 provides a summary of all CT and DCB test data. The resulting trend for the DCB tests was determined to be $G_{Ic} = 808\dot{\Delta}^{-0.107}$, while that for the CT tests (constant modulus) was

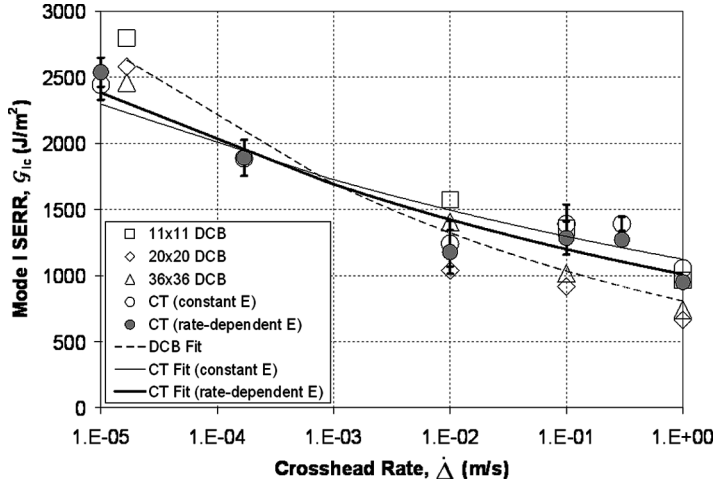


FIGURE 12 Average measured strain energy release rate values as a function of applied crosshead rate for CT and DCB test specimens. Error bars for two highest rates (*i.e.* 0.3 and 1 m/s) are so small that they are hidden for the CT test results. Error bars for DCB test results have been omitted for clarity. The legend refers to 11, 20, and 36 ply adherends used for the bonded DCB tests [7].

determined to be $G_{Ic} = 1124\dot{\Delta}^{-0.062}$ and that for the CT tests (rate-dependent modulus) was determined to be $G_{Ic} = 1010\dot{\Delta}^{-0.075}$ using a standard power law fit.

TTSP Correlation

The ability of a material to dissipate energy viscoelastically at small strain levels, as measured by $\tan \delta$, has often been correlated with strength and fracture properties of polymers [21–23]. Qualitative similarities are often seen, for example, as corresponding peaks in $\tan \delta$ and fracture toughness or fracture energy, since the same mechanisms that dissipate energy within the linear viscoelastic regime are expected to be present under the larger deformations that occur during fracture. In some cases, even quantitative agreement is observed [24], a fact that may be somewhat surprising considering the significant differences in deformation states that occur in small strain DMA tests and in the large scale deformations and post-yield conditions that occur during fracture events. In Fig. 13, the measured K_{Ic} (averaged for each specific test rate) from all tests conducted at room temperature is cross-plotted with the corresponding $\tan \delta$ for that condition. In order to correlate ramp-to-failure tests with sinusoidal DMA loading conditions, the time to failure of a fracture test is taken to be equivalent to $\pi/4$ of a cycle, thus equating the times to

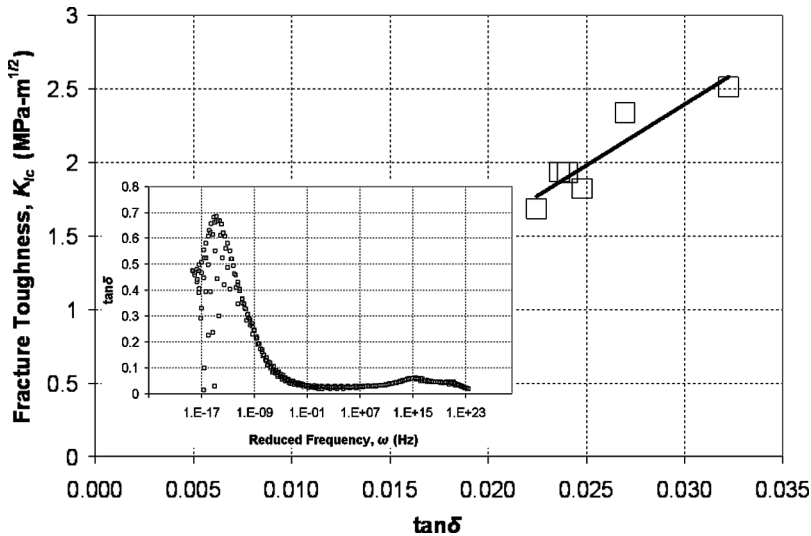


FIGURE 13 Variation of K_{Ic} with $\tan \delta$ for CT specimens [7].

peak load. The resulting relationship was determined to be $K_{Ic} = 83.2(\tan \delta) - 0.1$.

Subambient testing at temperatures -100°C below room temperature lowered K_{Ic} values to roughly 60% of the ambient values at a given applied crosshead rate. This is in relatively good agreement with the high-rate loading, where K_{Ic} values dropped to about 65% of the ambient temperature K_{Ic} as the crosshead rate was increased from quasi-static crosshead rates to 1 m/s. The TTSP suggests that high-rate tests are kinetically equivalent to colder tests conducted at slower rates, which has been quantitatively shown in Fig. 8 using DMA shift factors to shift the fracture data obtained at colder temperatures. The apparent ability of TTSP to account for the fracture toughness values obtained at subambient conditions is encouraging, as these tests are often easier to perform than dynamic tests, although additional testing is recommended to substantiate this correlation. Care should be taken with other material systems, however, as there are instances when TTSP is not applicable.

SUMMARY AND CONCLUSIONS

The fracture toughness of a commercial epoxy adhesive has been characterized using CT specimens tested over a range of temperatures and applied crosshead rates (up to 1 m/s) to gain insights into how this material might behave under low-speed impact conditions. At room temperature, the fracture toughness dropped steadily as crosshead rates were increased over six orders of magnitude, to values as low as 65% of the values obtained at slower rates. Attempts were made to test at effectively higher crosshead rates, in a TTSP sense, by conducting tests at subambient temperatures. Reductions in K_{Ic} were found at relatively low displacement rates for the subambient tests, and temperature effects on K_{Ic} were in good agreement with TTSP for this range of test rates.

Plastic zones, in the form of stress-whitened zones, were evident in all CT test specimens, becoming smaller as test speeds increased or temperatures decreased. Once the crack began to propagate, featureless failure surfaces were observed, suggesting that plastic deformation was significantly reduced for rapidly growing cracks. These results were consistent with significant stick-slip behavior observed in fracture tests of bonded specimens reported in a previous paper. The apparent ability of TTSP to describe adequately the K_{Ic} values at lower applied crosshead rates is encouraging. DMA tests are considerably easier to conduct than fracture tests, providing data over a range of frequencies and temperatures from a single specimen. The

encouraging correlation suggests that further insights into fracture results can be obtained with these simpler tests for this and other adhesive systems.

ACKNOWLEDGMENTS

The support of the Automotive Composites Consortium Energy Management Group is acknowledged. Finally, the authors also acknowledge that this research is supported in part by the U.S. Department of Energy (DOE) cooperative agreement number DE-FC05-95OR22363. Such support does not constitute an endorsement by the U.S. DOE of the views expressed herein. The authors would like to acknowledge Oak Ridge National Laboratory (ORNL) contributors including Ronny Lomax for preparing specimens, Rick Battiste for assistance with equipment, and Don Erdman for many of the instrumentation issues. In addition, several Virginia Tech individuals provided preliminary data related to this study, including Nathan Allison, Joshua Grohs, Joshua Simon, and Soojae Park, or collaborated with us on related modeling activities, including Dhaval Makhecha, Rakesh Kapania, and Eric Johnson.

The ORNL authors would like to acknowledge that this research was sponsored in part by the U.S. DOE, Assistant Secretary for Energy Efficiency and Renewable Energy, Office of Transportation Technologies, Lightweight Materials Program, under contract DE-AC05-00OR22725 with UT-Battelle, LLC. Accordingly, the U.S. Government retains a nonexclusive, royalty-free license to publish or reproduce the published form of this contribution, or allow others to do so, for U.S. Government purposes.

REFERENCES

- [1] Williams, J. G., *Fracture Mechanics of Polymers* (Ellis Horwood Limited, Chichester, 1984).
- [2] Williams, J. G. and Pavan, A. (Eds.), *Impact and Dynamic Fracture of Polymers and Composites, ESIS Publication 19* (Mechanical Engineering Publications Limited, London, 1995).
- [3] Freund, L. B., *Dynamic Fracture Mechanics* (Cambridge University Press, Cambridge, 1990).
- [4] Béguelin, P. and Kausch, H. H., A technique for studying the fracture of polymers from low to high loading rates, in *Impact and Dynamic Fracture of Polymers and Composites*, J. G. Williams and A. Pavan (Eds.) (Mechanical Engineering Publications Limited, London, 1995), pp. 3–19.
- [5] Plummer, C. J. G., Mauger, M., Béguelin, P., Orange, G., and Varlet, J., *Polymer* **45**(4), 1147–1157 (2004).

- [6] Simón, J. C., Johnson, E., and Dillard, D. A., *J. ASTM International* **2**, 53–71 (2005).
- [7] Pohlit, D. J., “Dynamic mixed-mode fracture of bonded composite joints for automotive crashworthiness,” Master’s Thesis, Virginia Tech, Blacksburg, VA (2007).
- [8] Dillard, D. A., Jacob, G.C., Pohlit, D. J., and Starbuck, J.M., “On the use of a driven wedge test to acquire dynamic fracture energies of bonded beam specimens: Part I – motivation and experimental implementation,” *J. Adhesion*, In preparation.
- [9] Pohlit, D. J., Dillard, D. A., and Starbuck, J. M., “Mixed-mode dynamic fracture testing of bonded composite beams,” *J. Adhesion*, In preparation.
- [10] Pohlit, D. J., Dillard, D. A., Starbuck, J.M., and Kapania, R., “On the use of a driven wedge test to acquire dynamic fracture energies of bonded beam specimens: Part II – finite element analysis,” *J. Adhesion*, In preparation.
- [11] Ferry, J. D., *Viscoelastic Properties of Polymers* (Wiley, New York, 1980), 3rd ed.
- [12] Kinloch, A. J., *Adhesion and Adhesives: Science and Technology* (Chapman and Hall, London, 1987).
- [13] Kinloch, A. J. and Young, R. J., *Fracture Behavior of Polymers* (Applied Science Publishers, London, 1983).
- [14] ASTM-D5045-99, “Standard test methods for plane strain fracture toughness and strain energy release rate of plastic materials,” in *Annual Book of ASTM Standards* (ASTM, West Conshohocken, PA, 1999).
- [15] Xiao, K. Q., Ye, L., and Kwok, Y. S., *J. Materials Science* **33**(11), 2831–2836 (1998).
- [16] Smiley, A. J. and Pipes, R. B., *J. of Composite Materials* **21**(7), 670–687 (1987).
- [17] Starbuck, J. M., Jacob, G. C., and Dillard, D. A., “Dynamic testing for quantifying rate sensitivities in bonded composite structures,” *Proceedings of the 2005 Society for Experimental Mechanics Annual Conference and Exposition*, Portland, OR, June 2005. Experimental and Applied Mechanics, Portland, OR.
- [18] Kanninen, M. F., *International J. Fracture* **9**, 83–92 (1973).
- [19] Kanninen, M. F., *International J. Fracture* **10**(3), 415–430 (1974).
- [20] Kinloch, A. J. and Shaw, S. J., *J. Adhesion* **12**, 59–77 (1981).
- [21] Bascom, W. D. and Cottingham, R. L., *J. Adhesion* **7**(4), 333–346 (1976).
- [22] Xu, S. Y. and Dillard, D. A., *IEEE Transactions on Components and Packaging Technologies* **26**(3), 554–562 (2003).
- [23] Han, J. C., Yang, Y. M., Li, B. Y., Wang, X. H., and Feng, Z. L., *J. Applied Polymer Science* **56**(9), 1059–1063 (1995).
- [24] Kamyab, I. and Andrews, E. H., *J. Adhesion* **56**(1–4), 121–134 (1996).